Electromagnetic properties of the isotones with $N = 50$ with the p35-i3 Hamiltonian

J. A. Purcell[1] and B. A. Brown[1]

[1] *Department of Physics and Astronomy, Michigan State University, East Lansing, Michigan 48824-1321, USA and Facility for Rare Isotope Beams, Michigan State University, East Lansing, Michigan 48824-1321, USA*

INTRODUCTION

The properties of the isotones with with $N = 50$ have historically been testing ground for shell-model configuration interaction (CI) calculations.

We consider the electromagnetic data for low-lying states of nuclei between ^{78}Ni and ^{100}Sn that can be described by protons in $(0f_{5/2}, 1p_{3/2}, 1p_{1/2}, 0g_{9/2}$ (the $\pi j4$ model space). The region between ^{90}Zr and ^{100}Sn is well established territory where many wavefunctions are dominated by $(1p_{1/2}, 0g_{9/2})$ orbitals [1], [2], [3], [4], [5], [6], [7]. The full $\pi j4$ space has been considered previously with Hamiltonians derived with the singular-valued decomposition method (SVD) [8], [9], [10], as well as those obtained VS-IMSRG methods [11]. This paper is based on set of newly derived SVD Hamiltonians called p30-i3, p35-i2 and p35-i3 [12]. In the notation px-iy, x stands for the number of SVD parameters and y stands for the ab-initio starting points used in [12].

The starting point for the Hamiltonians in derived in [12] are those obtained with the VS-IMSRG method. These are obtained using the EM 1.8/2.0 NN+3N interaction [13] in a harmonic oscillator basis with frequency $\hbar\omega = 12$ MeV, truncated to 13 major shells ($2n + l \leq e_{\max} = 12$). We normal order with respect to the Hartree-Fock ground state of the reference and discard the residual 3N interaction. We then decouple the $\pi j4$ valence space, using the Magnus formulation of the IMSRG. The results obtained with the standard approximation [14], truncating all operators at the two-body level throughout the flow, including inside nested commutators are labeled IMSRG(2) in [12]. The Hamiltnoians obtained with the SVD method starting with IMSRG(2) are are labeled $i2$.

Another starting point labeled IMSRG(3f2) in [12] introduces a correction in which intermediate three-body operators arising in nested commutators are incorporated by rewriting the double commutator in a factorized form while maintaining the same computational scaling as the IMSRG(2) approximation [15]. As in ref. [15], we include factorized terms with a one-body intermediate during the flow, and include terms with a two-body intermediate at the end of the flow. We perform the procedure for two different references, ^{78}Ni and ^{100}Sn, corresponding to empty and full valence spaces, respectively, and take the average of the two resulting valence space Hamiltonians as our starting point for the fitting procedure. The Hamiltnoians obtained with the SVD method with starting with IMSRG(3f2) are are labeled $i3$.

We showed in [12] that the IMSRG(3f2) provided a better starting point for describing the experimental energy data in the sense that the rms deviation obtained with $p < 10$ SVD parameters was much smaller with IMSRG(3f2) compared to IMSRG(2). Thus, IMSRG(3f2) might provide a better input for the linear combinations of $69 - p$ SVD parameters that are not well determined from experimental data.

In [12] we showed that the optimal number number of SVD parameters was about $p = 35$ based on the minimum in the rms deviations in trial sets of data. For the purpose of investigating the Hamiltonian uncertainties in the observables we also obtained a Hamiltonian with $p = 30$ SVD parameters.

ELECTROMAGNETIC OBSERVABLES

One can express the one-body reduced matrix element for the n-particle wave function in the form of a product over one-body transition densities (OBTD) times reduced single-particle matrix elements (SPME) $< k_\alpha||O^\lambda||k_\beta >$

$$< f||\hat{O}^\lambda||i > =< n\omega_f J_f||\hat{O}^\lambda||n\omega_i J_i >$$

$$= \sum_{k_\alpha k_\beta} \mathrm{OBTD}(fik_\alpha k_\beta\lambda) < k_\alpha||O^\lambda||k_\beta >, \qquad (1)$$

where the OBTD is given by

$$\mathrm{OBTD}(fik_\alpha k_\beta\lambda) = \frac{< n\omega_f J_f||[a^+_{k_\alpha} \otimes \tilde{a}_{k_\beta}]^\lambda||n\omega_i J_i >}{\sqrt{(2\lambda+1)}}. \qquad (2)$$

The labels i and f are a shorthand notation for the initial and final state quantum numbers $(n\omega_f J_f)$ and $(n\omega_i J_i)$, respectively. The k_α label the spherical single-particle states (n, ℓ, j) used in the model space. The NuShellX code [16] provides the wavefunctions and the resulting OBTD.

The $< k_\alpha||O^\lambda||k_\beta >$ are the SPME obtained with the $E\lambda$ and $M\lambda$ operators. We consider magnetic moments

$$\mu = \sqrt{\frac{4\pi}{3}} < i, J, M = J \mid \hat{O}(M1) \mid i, J, M = J >$$

$$= \sqrt{\frac{4\pi}{3}} \begin{pmatrix} J & 1 & J \\ -J & 0 & J \end{pmatrix} < i, J||\hat{O}(M1)||i, J >, \qquad (3)$$

quadrupole moments

$$Q = \sqrt{\frac{16\pi}{5}} < J, M = J \mid \hat{O}(E2) \mid J, M = J >$$

$$= \sqrt{\frac{16\pi}{5}} \begin{pmatrix} J & 2 & J \\ -J & 0 & J \end{pmatrix} < i, J||\hat{O}(E2)||i, J >, \quad (4)$$

and reduced transition probabilities

$$B(O^\lambda, i \to f) = \frac{|< f||\hat{O}^\lambda||i >|^2}{2J_i + 1} \quad (5)$$

We consider mainly the B(M1) and B(E2) with the standard form of the SPME as given in [17]. B(E1) are zero since the parity-changing λ=1 operator does not connect any of the orbitals in the $j4$ model space. B(M2) are not considered since the parity-changing λ=2 operator it limited to only one, $0g_{9/2} - 1f_{5/2}$, of the 10 SPME with one orbital in the $j4$ model space involved in M2 transitions. We have a short section on B(E3) as observed in inelastic scattering experiment.

For $M1$ the SPME involve spin and orbital g-factors which are usually treated as effective parameters to take into account configuration mixing outside the $j44$ model space and mesonic-exchange currents. We use the orbital-dependent effective g-factors obtained from fits to data in [17]. For $E2$ the SPME involve radial integrals. It is common to harmonic-oscillator radial wavefunctions. For example, a value of $b^2 = 4.481$ for the oscillator parameter was used in [17]. In addition, one uses an effective proton charge e_p to take into account mixing with configurations that are not included in the $j4$ model space. In [17] a value of $e_p = 2.0$ was needed with their harmonic-oscillator radial wavefunction assumption. It is better to use more realistic nucleus-dependent radial wavefunctions obtained with energy-density functionals (EDF). For this purpose we use the Skx Skyrme functional [18]. With this EDF a value of $e_p = 1.8$ gives a good reproduction of all of the $E2$ data we consider (see Sec. ?).

UNCERTAINTIES RELATED TO THE CHOICE OF HAMILTONIAN

Here we compare global sets of electromagnetic observables obtained with the new p35-i3, p35-i3 and p30-i3 Hamiltonians together with older Hamiltonians, jun45 [8], and jj44a [10]. The purpose is to use these comparisons to deduce Hamiltonian uncertainties in the observables. We note that all of these Hamiltonians are based on fits to data in the $\pi j4$ model space, except for jun45 which is based on a fit to data in larger proton-neutron $jj44$ model space.

We calculated observables for all nuclei between ^{80}Zn and ^{98}Cd and divided for results into those for nuclei with $A < 88$ and those for nuclei with $A \geq 88$. The wavefunctions for low-lying states with $A < 88$ are dominated by the three orbitals ($0f_{5/2}, 1p_{3/2}, 1p_{1/2}$ and those with $A \geq 88$ are dominated by the two orbitals ($1p_{1/2}, 0g_{9/2}$). It was found in [12] that rms deviation between experiment and theory for the binding energies excitation energies was significantly larger in the first group (0.12 MeV). than those in the second groop (0.05 MeV). Thus, we can anticipate that the rms deviations in the various observables will be larger in the first group compared to the those in the second group.

For each Hamiltonian we calculated the magnetic and quadrupole moments for the first state of each J^π. Also we calculated the B(M1) and B(E2) for the first state of each J^π with the first state $(J+2)^\pi$ We did not include those for which the states were less that 200 keV from the second state with the same J^π. For set of each set of comparisons we give the rms differences in the specific observables. These values are indicative of the associated theoretical uncertainties.

We show the comparison of results obtained with the IMSRG(3f2) starting Hamiltonian for two different values of the number of VLC linear combinations varied (30 and 35) in Figs. 1 and 2. As expected the rms difference is always larger for nuclei $A < 88$ compared to those for $A \geq 88$. For the moments (Fig. 1) and B(E2) (Fig. 2-cd) this difference is about a factor of two. For the B(M1) the difference is much larger. The reason is that the small B(M1) (WU = 1.79 μ_N^2) arise from cancellations between components in Eq. (1) which are particularly sensitive to small changes in the Hamiltonian.

We find a particular outlier for the B(E2) in Fig. 2c with (p30-i3,p35-i3) values of (4,142) e^2 fm^4. This comes from the $7/2_1^-$ to $3/2_1^-$ transition in ^{81}Ga. As seen in Fig. 9 of [12], there are two low-lying $3/2^-$ states in ^{81}Ga. The B(E2) for the $7/2_1^-$ to $3/2_2^-$ transition are (74,8) e^2 fm^4. It is not clear what part of the Hamiltonian is responsible for the interchange of properties for these B(E2) transitions.

The calculated gamma-decay branching of the $7/2^-$ state to the ($3/2_1^-$,$5/2_1^-$) states is (25,75)% for p35i3 and (1,99)% for p30i3. The gamma-decay data of [19] gives (0,100)% for the state at 1.40 MeV. Assuming this is the $7/2^-$ state, the data is in agreement with the p30i3 Hamiltonian result.

We show the comparison of results obtained with the IMSRG(2)and IMSRG(3f2) starting Hamiltonian for 35 varied VLC linear combinations, (p35-i2) and (p35-i3), respectively in Figs. 3 and 4. The scatter and rms deviations are similar to the (p30-i2) and (p35-i3) comparisons discussed above.

The jj44a Hamiltonian [10] was obtained from a fit to the $N = 50$ energy data as known in the year 2004. The comparison of electromagnetic results obtained with jj44a and p35-i3 are shown in Fig. 5 and 6. The scatter is significantly worse compared to the previous compar-

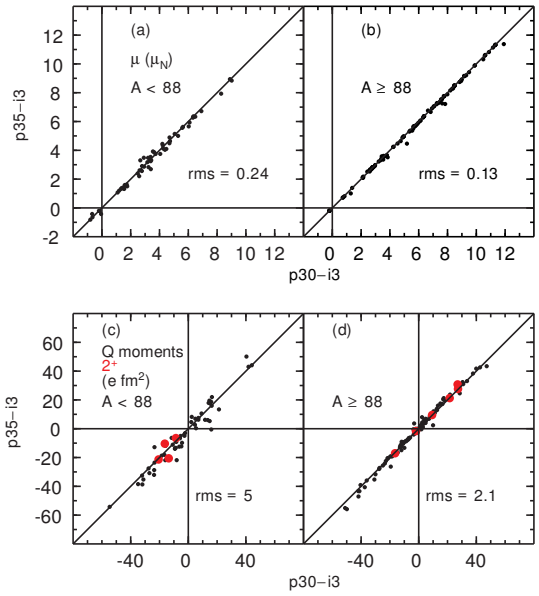

FIG. 1: Comparison of moments obtained with the p30-i3 and p35-i3 Hamiltonians.

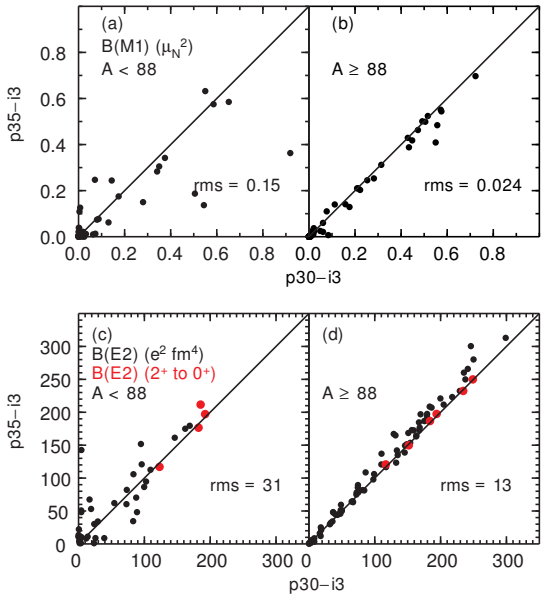

FIG. 2: Comparison of B(M1) and B(E2) values obtained with the p30-i3 and p35-i3 Hamiltonians.

isons, particularly for the B(M1) and B(E2) in Fig. 6.

Finally, in Figs. 7 and 8 we show the comparison of the electromagnetic results obtained with the jun45 Hamiltonian compared to p35-i3. The scatter is much worse. This reflects the fact that the jun45 Hamiltonian was obtained from a much wider set of nuclei. In particular, the $T = 1$ part of the jun45 Hamiltonian is influenced by data for the nickel isotopes. In [10] differences in the $T = 1$ Hamiltonians obtained from the $N = 50$ isotones and the $Z = 28$ isotopes were discussed. In particular, the relatively lower energy of 2^+ states in $^{70-78}$Ni compared to those in ^{92}Mo-^{98}Cd results in the inversion of seniority two and four states in $^{72-76}$Ni compared to ^{94}Mo-^{96}Cd. Thus, one concludes that "universal-type" Hamiltonians are useful, but one can do better with local Hamiltonians designed from a specific range of nuclei. Ultimately one should consider and construct nucleus-dependent Hamiltonians in the spirit of VS-IMSRG calculations [14].

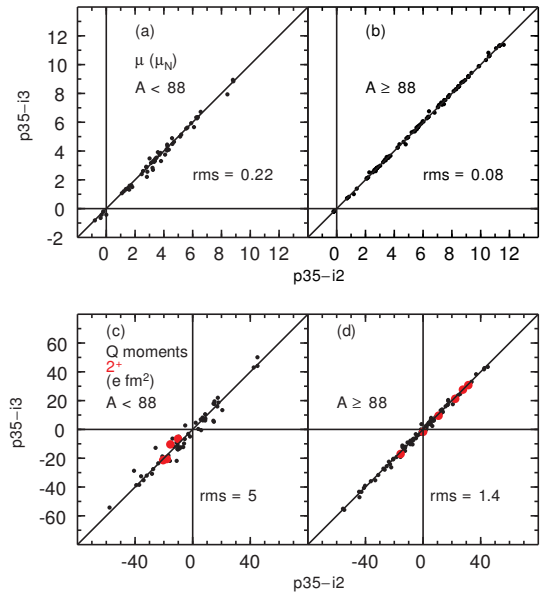

FIG. 3: Comparison of moments obtained with the p35-i2 and p35-i3 Hamiltonians.

COMPARISON BETWEEN THEORY AND EXPERIMENT

Jordan will add his figures and discussion here

CONFIGURATION WITH j^n

Will modify this section

For states with good seniority the $B(E2)$ between j^n configurations with ν=2 is given by [20]

$$B(E2)(j^n, J_i \to J_f) = \left[\frac{2j+1-2n}{2j+1-2\nu}\right]^2 B(E2)(j^2, J_i \to J_f).$$

For example, for $j = 9/2$ and $n = 4$ (or $n = 6$)

$$B(E2, j^4, \nu = 2) = (1/9)B(E2, j^2, \nu = 2).$$

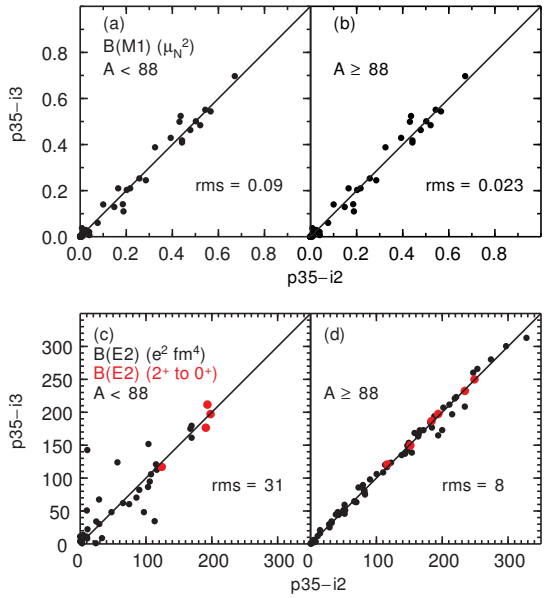

FIG. 4: Comparison of B(M1) and B(E2) values obtained with the p35-i2 and p35-i3 Hamiltonians.

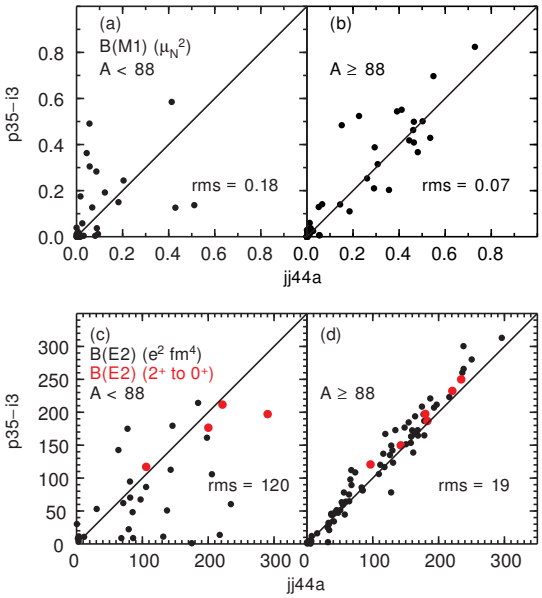

FIG. 6: Comparison of B(M1) and B(E2) values obtained with the jj44a and p35-i3 Hamiltonians.

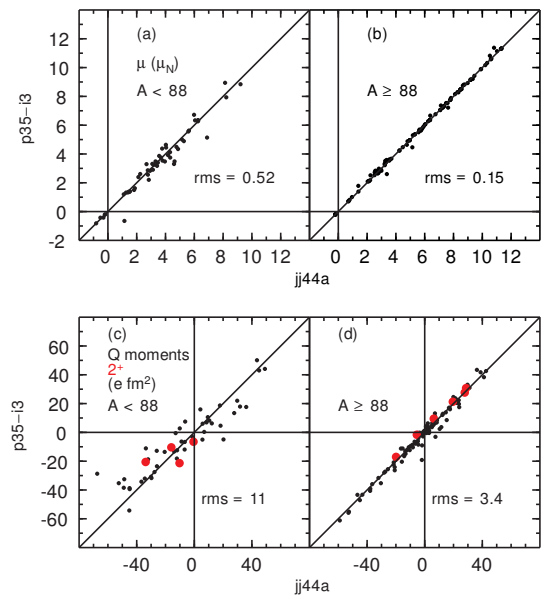

FIG. 5: Comparison of moments obtained with the jj44a and p35-i3 Hamiltonians.

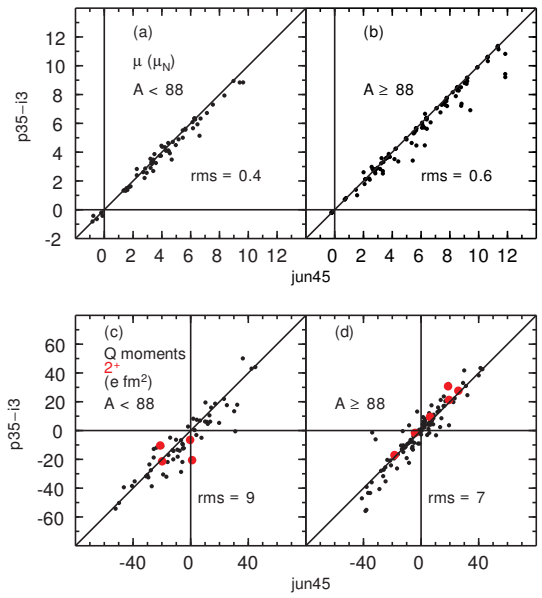

FIG. 7: Comparison of moments obtained with the jun45 and p35-i3 Hamiltonians.

ACKNOWLEDGEMENTS

We acknowledge support from the National Science Foundation grant PHY-2110365.

[1] I. Talmi and I. Unna, Nucl. Phys. **19**, 225 (1960).
[2] S. Cohen, R. D. Lawson, M. H. Macfarlane, and M. Soga, Phys. Lett. **10**, 195 (1964).
[3] N. Auerbach and I. Talmi, Nucl. Phys. **64**, 458 (1965).
[4] J. Vervier, Nucl. Phys. **75**, 17 (1966).

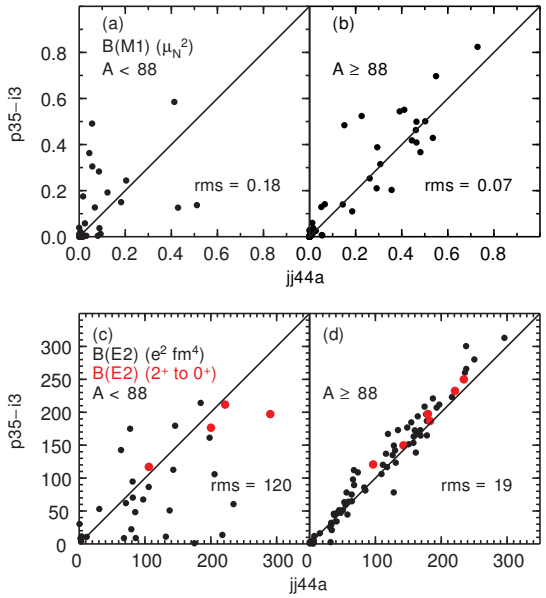

FIG. 8: Comparison of B(M1) and B(E2) values obtained with the jun45 and p35-i3 Hamiltonians.

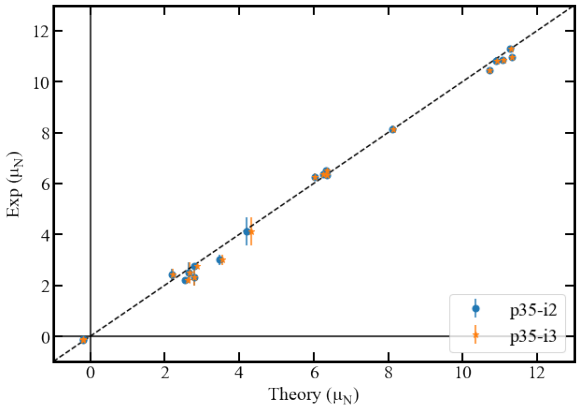

FIG. 9

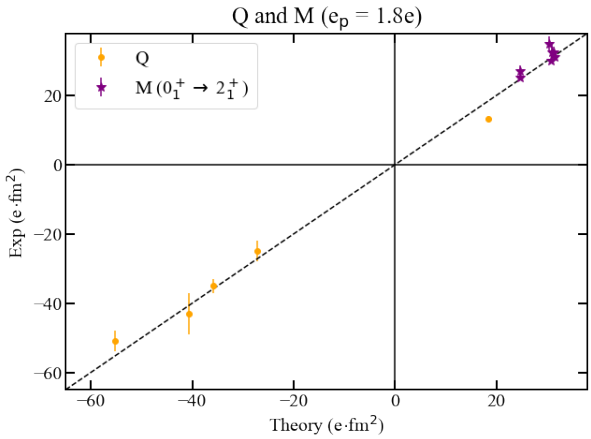

FIG. 10

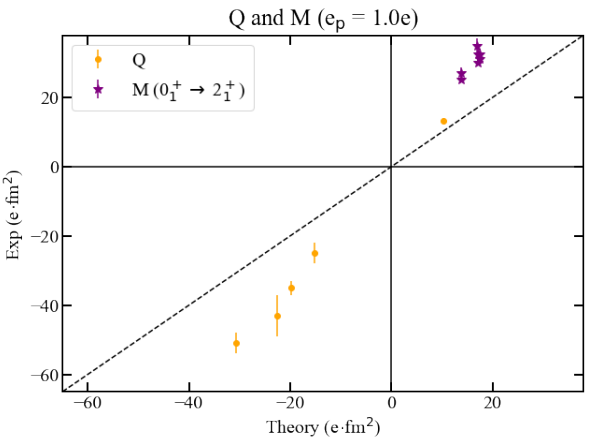

FIG. 11

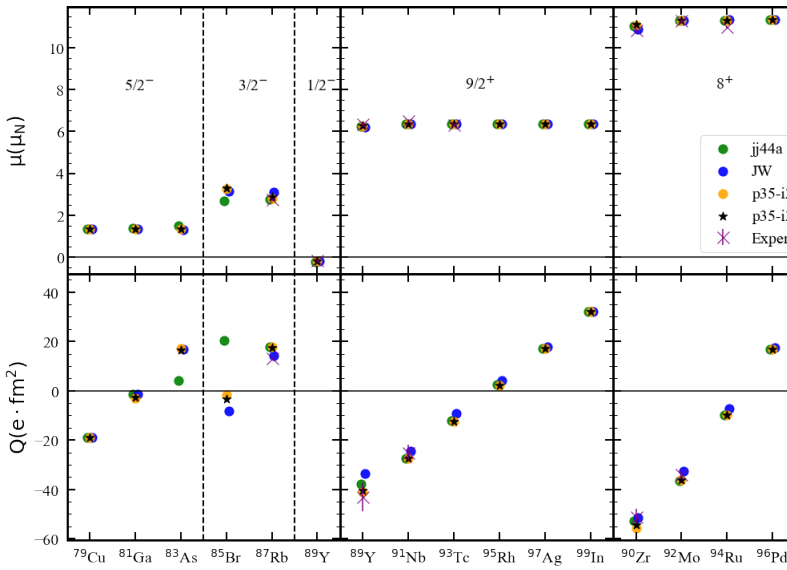

FIG. 12

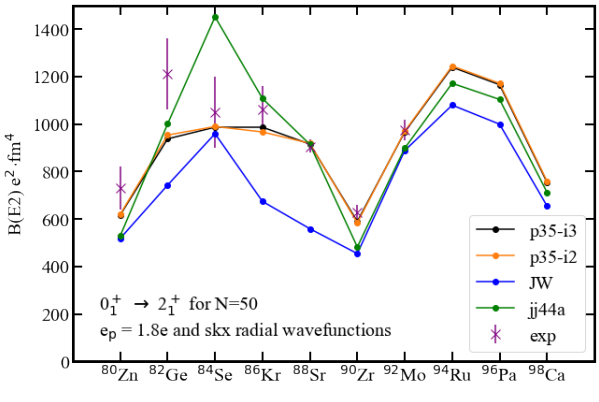

FIG. 13

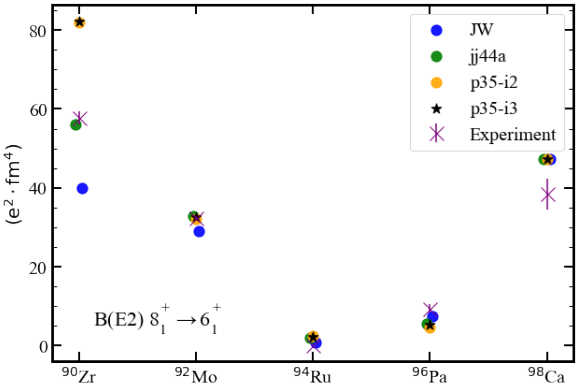

FIG. 14

[5] J. B. Ball, J. B.McGrory, and J. S. Larsen, Phys. Lett. **41B**, 581 (1972).

[6] D. H. Gloeckner and F. J. D. Serduke, Nucl. Phys . **A220**, 4 (1973).

[7] J. Blomqvist and L. Rysdtrom, Phys. Scr. **31**, 31 (1985).

[8] M. Honma, T. Otsuka, T. Mizusaki, and M. Hjorth-Je nsen, Phys. Rev. C **80**, 064323 (2009).

[9] X. Ji and B. H. Wildenthal, Phys. Rev. C **37**, 1256 (1988).

[10] A. F. Lisetskiy, B. A. Brown, M. Horoi and H. Grawe, Phys. Rev. C **70**, 044314 (2004).

[11] Q. Yuan and B. S. Hu, Phys. Lett. B **858**, 139018 (2024).

[12] J. A. Purcell, B. A. Brown, B. C. He, S. R. Strober g, and W. B. Walters, Phys. Rev. C **111**, 044313 (2025).

[13] K. Hebeler, S. K. Bogner, R. J. Furnstahl, A. Nogga, and A. Schwenk Phys. Rev. C **83**, 031301(R) (2011)

[14] S. R. Stroberg, H. Hergert, S. K. Bogner, and J. D. Holt, Annu. Rev. Nucl. Part. Sci. 2019. **69**, 307 (2019).

[15] B. C. He and S. R. Stroberg, Phys. Rev. C **110**, 044317 (2024).

[16] B. A. Brown and W. D. M. Rae, Nuclear Data Sheet s **120**, 115 (2014).

[17] X. Ji and B. H. Wildenthal, Phys. Rev. C **38**, 2849 (1988).

[18] B. A. Brown, Phys. Rev. C **58**, 220 (1998).

[19] V. Paziy *et al.*, Phys. Rev. C **102**, 014329 (2020).

[20] B. Maheshwari and K. Nomura, Symmetry **14**, 2680 (2022).